

# Isotropic cosmic birefringence from string axion domain walls without cosmic strings, and DESI results

Junseok Lee<sup>1</sup>, Kai Murai<sup>1</sup>, Fuminobu Takahashi<sup>1</sup>, Wen Yin<sup>2</sup>

<sup>1</sup>*Department of Physics, Tohoku University, Sendai, Miyagi 980-8578, Japan*

<sup>2</sup>*Department of Physics, Tokyo Metropolitan University, Tokyo 192-0397, Japan*

## Abstract

Recently, the Atacama Cosmology Telescope (ACT) DR6 results showed a preference for isotropic cosmic birefringence, which is consistent with the previous analyses using the Planck and WMAP data. Independently, the Dark Energy Spectroscopic Instrument (DESI) DR2 results further support that dark energy is evolving over the history of the universe, enhancing the possibility of new physics in the late-time universe. In this paper, we propose that if domain walls associated with the string axion are formed, the isotropic cosmic birefringence can be explained naturally. Interestingly, avoiding the domain wall problem, the domain wall formation is predicted to be much later than the epoch of recombination. Compared with the previous proposal of kilobyte cosmic birefringence, where domain wall formation occurs before recombination, the predicted rotation angle,  $\beta \approx 0.21c_\gamma \text{ deg}$  with the anomaly coefficient  $c_\gamma \approx 1$ , does not suffer from the ambiguity of the population bias. The prediction is in excellent agreement with the ACT (and combined) data regarding cosmic birefringence. This scenario can be probed from the anisotropic birefringence for the photons emitted well after the recombination and the gravitational waves. In addition, the late-time dynamics of the axion contributes to the dark energy component, and we also study the relation to the DESI results.

# 1 Introduction

Light axions may be ubiquitous in nature. In string or M theory, numerous axions commonly appear, which we collectively denote by  $\phi$ . Their cosmological and phenomenological implications have been investigated in the contexts of the axiverse or axion landscape scenarios [1–8]. The axion exhibits a discrete shift symmetry,

$$\phi \rightarrow \phi + 2\pi f_\phi, \quad (1)$$

where  $f_\phi$  is the axion decay constant. Unless one considers large-volume compactification, the string axion has the decay constant of

$$f_\phi = 10^{15} - 10^{17} \text{ GeV}. \quad (2)$$

Typically, the axion potential is generated via non-perturbative effects, and its mass can be exponentially suppressed. A distinctive prediction of theories involving axions is the existence of degenerate vacua; if these degenerate vacua are realized in the universe, they are separated by domain walls.

The axion may also couple to photons through an anomaly as

$$\mathcal{L} = c_\gamma \frac{\alpha}{4\pi} \frac{\phi}{f_\phi} F_{\mu\nu} \tilde{F}^{\mu\nu} \equiv \frac{1}{4} g_{\phi\gamma\gamma} \phi F_{\mu\nu} \tilde{F}^{\mu\nu}, \quad (3)$$

where  $c_\gamma$  is an anomaly coefficient,  $\alpha$  is the fine structure constant, and  $F_{\mu\nu}$  together with  $\tilde{F}_{\mu\nu}$  denote the field strength and its dual, respectively. In the literature, an axion with such a coupling to photons is often referred to as an axion-like particle (ALP). For reviews on axions and related topics, see Refs. [9–15]. The axion photon coupling is constrained as  $g_{\phi\gamma\gamma} < 6.3 \times 10^{-13} \text{ GeV}^{-1}$  for axions lighter than  $10^{-12} \text{ eV}$  [16], which gives  $f_\phi > 3.7 \times 10^9 c_\gamma \text{ GeV}$ .

Recently, a hint of isotropic cosmic birefringence (CB) in the cosmic microwave background (CMB) polarization was reported, with a rotation angle given by [17],

$$\beta = 0.20 \pm 0.08 \text{ deg}, \quad (4)$$

based on an analysis of the ACT DR6 polarization data. This is consistent with the previous analyses of the Planck and WMAP data  $\beta = 0.34 \pm 0.09 \text{ deg}$  [18] (see also Refs. [19–22]). Assuming independence, we combine them and obtain

$$\beta^{\text{combined}} = 0.26 \pm 0.06 \text{ deg}, \quad (5)$$

achieving an excess greater than  $4\sigma$ .

One plausible mechanism to generate this CB is to introduce an ALP that varies temporally and/or spatially [4, 23–54] (see also Ref. [55] for a review). When a photon propagates through a slowly varying ALP background, its polarization angle  $\Phi$  evolves as [56–58]

$$\dot{\Phi} \approx \frac{c_\gamma \alpha}{2\pi} \frac{\hat{r}^\mu \partial_\mu \phi}{f_\phi}, \quad (6)$$

where the dot denotes a derivative with respect to the time along the photon trajectory, and  $\hat{r}^\mu$  represents the normalized photon four-momentum; for example,  $\hat{r} = (1, 0, 0, 1)$  when the photon travels in the positive  $z$  direction. By integrating this equation along the line of sight from the last scattering surface (LSS) to the observer, one obtains a net rotation of the polarization plane,

$$\Delta\Phi(\Omega) = 0.42 \text{ deg} \times c_\gamma \left( \frac{\phi_{\text{today}} - \phi_{\text{LSS}}(\Omega)}{2\pi f_\phi} \right), \quad (7)$$

where  $\phi_{\text{today}}$  and  $\phi_{\text{LSS}}(\Omega)$  denote the axion field values at the solar system today and at the LSS, respectively, and  $\Omega$  specifies the angular direction in polar coordinates  $(\theta, \varphi)$ . The isotropic CB angle is then given by

$$\beta = \frac{1}{4\pi} \int d\Omega \Delta\Phi(\Omega). \quad (8)$$

If the change in the axion field value exactly matches the discrete shift symmetry transformation (1), i.e., if  $\phi_{\text{today}} - \phi_{\text{LSS}}(\Omega) = 2\pi f_\phi$ , then the rotation angle becomes  $\beta = 0.42 c_\gamma \text{ deg}$ , which is intriguingly close to the observed value (4) for  $c_\gamma = \mathcal{O}(1)$ . This coincidence motivates our study of the CB induced by axion domain walls that separate adjacent vacua related by the periodicity (1).

In particular, it was proposed by the present authors in Ref. [29] that the reported value of the rotation angle can be explained by the ALP domain wall in the scaling solution. This is because the observation around Earth is in a single domain while the domain wall in the recombination has the  $10^{3-4}$  domains on the LSS, the field value averages to the mean value of two adjacent vacua. Depending on which vacuum the axion occupies in a given domain, the rotation angle  $\Delta\Phi(\Omega)$  will take one of two possible values—either zero or  $0.42 c_\gamma \text{ deg}$ . Consequently, the CB from each domain encodes one bit of information, hence the term the kilobyte cosmic birefringence (KBCB). The isotropic one is predicted by the average,

$$\beta \approx 0.21 c_\gamma \text{ deg}, \quad (9)$$

irrelevant to the decay constant. Indeed the domain wall network from inflationary fluctuations is stable under the population bias [39]. Surprisingly this value with  $c_\gamma \sim 1$  agrees well with the measurement Eq. (4) and also the combined ones depending on  $c_\gamma$ .

Since the domain wall is between the adjacent equivalent minima related by Eq. (1), one cannot employ the potential bias to resolve the domain wall problem. From the absence of the domain wall problem with a formation prior to the recombination, the KBCB scenario requires the axion to have a decay constant of  $f_a \ll 10^{15}$  GeV, which is out of the typical range for string axions and requires the explanation of the origin of the ALP. In addition, although the domain wall is stable under the population bias, the population bias may change the prediction for  $\beta$  because the averaging to  $0.42c_\gamma/2$  deg is not precise.

In this paper, we study the possibility that the domain wall from a string axion explains the isotropic CB. We show that the formation of the domain wall with the decay constant (2) must occur after the recombination to avoid the domain wall problem. In this case, there is only highly suppressed ambiguity of the prediction given  $c_\gamma$  and the potential shape. Furthermore, depending on the parameter region, we may have predictions of anisotropic CB corresponding to the photons from a later epoch (e.g. reionization photons), gravitational waves, and the CMB anisotropies.

On the other hand, Dark Energy Spectroscopic Instrument (DESI) DR2 baryonic acoustic oscillation measurements [59, 60], with a larger and higher-quality dataset than DR1 [61], improve statistical precision by about 40%. Combined with the CMB and supernova data [62, 63], these results provide stronger hints ( $2.8\sigma - 4.2\sigma$ ) for a time-dependent dark energy component over a cosmological constant. The explanations for these results have been studied in Refs. [64–72]. For instance, the time-varying dark energy to explain the cosmic birefringence was discussed in Refs. [64, 65] (see also Ref. [32] before the DESI data release, as well as more earlier papers [73, 74]). Such time-varying dark energy may be related to the cosmological constant problem [65, 75]. Indeed, the time-varying dark energy was predicted in the model for alleviating the cosmological constant problem [75]. In terms of the DESI DR2, a hilltop axion model with matter effects to simultaneously alleviate the  $S_8$  tension was studied [76] (see a similar model [39] for domain wall formation and Refs. [77–82] for more generic realizations of a hilltop axion). Since our model predicts the late-time formation of domain walls, we study the contribution to the time-dependent dark energy component.

## 2 String Axion Domain Walls without Strings and Isotropic Cosmic Birefringence

In this section, we demonstrate that domain walls can form without strings by employing a simple model, and we clarify the necessary conditions for this mechanism to operate. For

our purposes, it is sufficient to consider the following potential:

$$\begin{aligned}
V(\phi) &= \Lambda^4 \left[ 1 + \cos \left( \frac{\phi}{f_\phi} \right) \right] \\
&\simeq 2\Lambda^4 - \frac{1}{2}m_\phi^2\phi^2 + \frac{1}{4} \left( \frac{\Lambda}{f_\phi} \right)^4 \phi^4 + \dots,
\end{aligned}
\tag{10}$$

where  $\Lambda$  is a dynamical scale,  $m_\phi \equiv \Lambda^2/f_\phi$  is the mass (or curvature) of the axion, and the potential is expanded around the origin in the second equality. This potential is invariant under the discrete shift symmetry (1), and as a consequence, it possesses degenerate vacua.

Let us assume that during inflation the axion is (nearly) massless, i.e.,  $H_{\text{inf}} \gg m_\phi$ , where  $H_{\text{inf}}$  is the Hubble parameter during inflation. In this case, the axion acquires quantum fluctuations of amplitude

$$\delta\phi = \frac{H_{\text{inf}}}{2\pi}$$

about a zero mode  $\phi_0$ , and these fluctuations become classical after horizon exit. Here, the zero mode is defined as the axion field value averaged over the observable universe. The superhorizon fluctuations accumulate in a random-walk fashion, and the variance of the (Gaussian) probability distribution of the axion field,  $\sigma_\phi^2$ , grows as

$$\sigma_\phi^2(N_e) = N_e \left( \frac{H_{\text{inf}}}{2\pi} \right)^2,$$

with  $N_e$  being the number of e-folds. After inflation, the axion begins to oscillate when the Hubble parameter drops to approximately

$$H_{\text{osc}} = m_\phi.$$

Suppose that  $\phi_0$  is sufficiently close to the origin such that

$$|\phi_0| \lesssim \sigma_\phi(N_{\text{osc}}), \tag{11}$$

where  $N_{\text{osc}}$  is the number of e-folds corresponding to the horizon exit of the mode with wavenumber  $k/a = H_{\text{osc}}$  during inflation. This condition, which is important for the scenario to work, will be justified later.

Since the probability distribution of the axion spans both sides of the potential maximum, domain walls are formed when the axion begins to oscillate. Although inflationary fluctuation naturally has the population bias, the large-scale correlation makes the network long-lived [39].

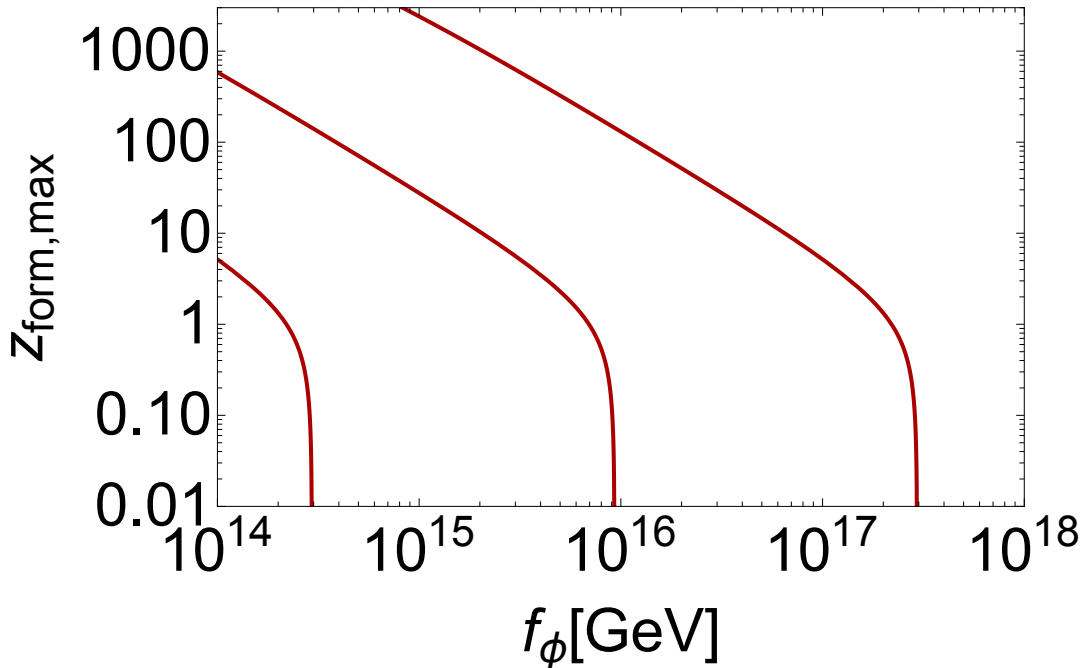


Figure 1: Maximal formation redshift for the string axion domain wall with  $\sigma_{\text{DW}} = (10 \text{ MeV})^3$ ,  $(1 \text{ MeV})^3$ , and  $(0.1 \text{ MeV})^3$  from top to bottom. Here we assume the fluctuation is of the order of unity to estimate the formation time (see Fig. 2 for the realistic case depending on the initial fluctuation). Given that the domain wall problem constrains  $\sigma \lesssim (1 \text{ MeV})^3$ , the domain wall formation well after recombination,  $z_{\text{form}} \lesssim 100$ , is required for  $f_a \simeq 10^{15} - 10^{16} \text{ GeV}$ .

The onset of the oscillation of the axion or the domain wall formation begins at

$$H \sim H_{\text{osc}} = m_\phi.$$

Note that this is the case when the fluctuation is not much smaller than  $f_a$  (see Fig. 2). From Eq. (2), we obtain the onset of oscillation as shown in Fig. 1. There is a domain wall problem unless the tension satisfies [83, 84],

$$\sigma_{\text{DW}} \simeq 8m_\phi f_\phi^2 \lesssim (1 \text{ MeV})^3, \quad (12)$$

where the first equality is for the potential (10). This bound is set by the constraint from the CMB temperature anisotropies induced by the gravitational potential of the domain walls. In the figure, we show the contour for  $\sigma_{\text{DW}} = (10 \text{ MeV})^3$ ,  $(1 \text{ MeV})^3$ , and  $(0.1 \text{ MeV})^3$  from top to bottom. The top one is for the conservative bound because our DW has population bias,

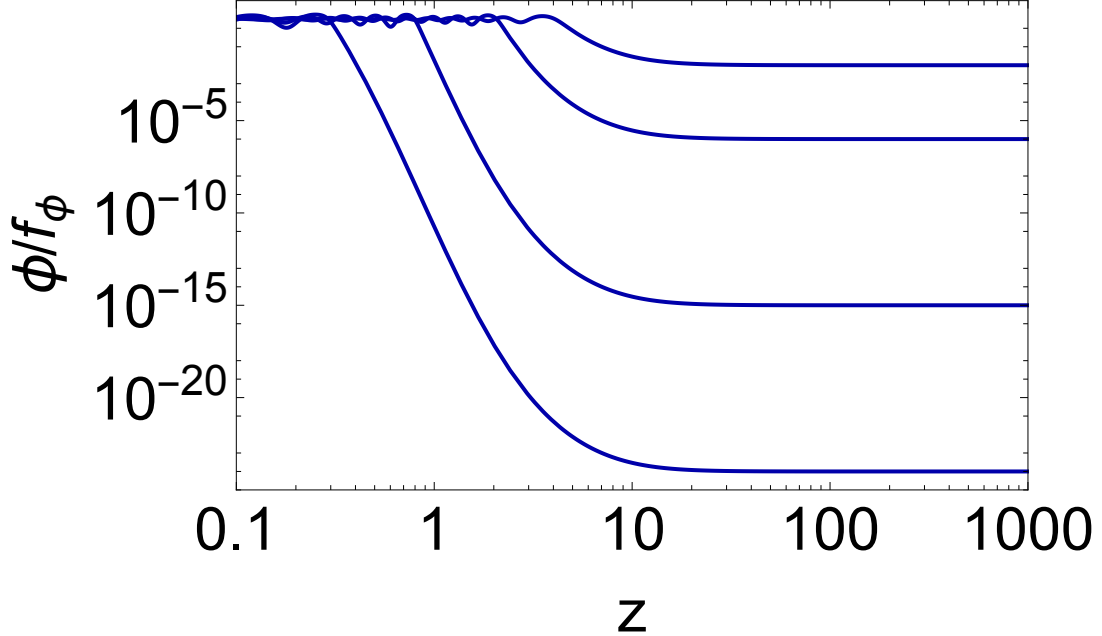


Figure 2:  $\phi$  field evolution with different initial conditions,  $\phi_{\text{ini}} = \{10^{-9}, 1, 10^9, 10^{13}\}$  GeV from bottom to top, which may be considered as  $\sim H_{\text{inf}}$ . The domain wall formation time can be read from the field evolution to  $\phi/f_\phi \sim \pi$ . We assume  $f_\phi = 10^{15}$  GeV and  $\sigma_{\text{DW}} = (1 \text{ MeV})^3$ .

is from inflationary fluctuation (e.g. the area parameter is half of the usual one even for the absence of the population bias [85]), and forms late, although we will adopt the bound for  $(1 \text{ MeV})^3$  in the paper. We therefore find that given that the domain wall problem constrains  $\sigma \lesssim (1 \text{ MeV})^3$ , the domain wall formation well after recombination,  $z_{\text{form}} \lesssim 100$ , is required for  $f_a \simeq 10^{15} - 10^{16}$  GeV.

Since  $H_{\text{inf}} \lesssim 10^{13}$  GeV from the current CMB bound [86–89] and Eq. (2), we obtain the recombination,

$$\frac{|\bar{\phi}_{\text{LSS}}|}{f_\phi} < \frac{\sigma_\phi}{f_\phi} \simeq \sqrt{N_e} \frac{H_{\text{inf}}}{2\pi f_\phi} \ll 1, \quad (13)$$

where  $\bar{\phi}_{\text{LSS}}$  is the average of  $\phi_{\text{LSS}}(\Omega)$  over the LSS. Since after the domain wall formation we are in either domain, we get the isotropic CB

$$\boxed{\beta = 0.42 \text{ deg} \times c_\gamma \left( \frac{\phi_{\text{today}} - \phi_{\text{LSS}}}{2\pi f_\phi} \right) \approx 0.21 \text{ deg} \times c_\gamma \left( \frac{\phi_{\text{today}}}{\pi f_\phi} \right)}. \quad (14)$$

Note that the dynamics for the isotropic CB is different from the original KBCB scenario,

where  $\bar{\phi}_{\text{LSS}} = (\phi_{\text{min},1} + \phi_{\text{min},2})/2$  with  $\phi_{\text{min},1}$  and  $\phi_{\text{min},2}$  being the field value of the adjacent minima, one of which is for our minimum.

To have the conditions of Eq. (11), we can consider some possibilities. One is the existence of many string axions predicted by string theory. For instance, for  $f_\phi = 10^{15}$  GeV and  $H_{\text{inf}} = 10^{13}$  GeV with 100 light axions, we naturally have one axion around the hilltop according to the stochastic distribution. Alternatively, we can consider the mixing between axions (or phases in Higgs) to realize the hilltop axion [77–82]. Another possibility is the matter effects to reverse the potential [39] (see also Ref. [76]).

We also mention that the formation time can be much later than the maximal one discussed in Fig. 1 in this scenario because the fluctuation is very small. This can be seen in Fig. 2, where we plot the motion of homogeneous  $\phi$ , which can be understood as the averaged  $\phi$  in a large enough domain. Here we solve the equation of motion

$$\left( (1+z)H \frac{d}{dz} \right)^2 \phi - 3H^2(1+z) \frac{d}{dz} \phi = -\partial_\phi V. \quad (15)$$

The initial condition is taken to be  $\phi_{\text{ini}} = \{10^{-9}, 1, 10^9, 10^{13}\}$  GeV, arranged from bottom to top with  $f_\phi = 10^{15}$  GeV and  $\sigma_{\text{DW}} = (1 \text{ MeV})^3$ . These initial conditions may be considered to be of the order of  $H_{\text{inf}}$ . The time of domain wall formation can be identified when the field evolution reaches  $\phi/f_\phi \sim \pi$ , where the field starts to oscillate.

We see that to avoid the domain wall problem for the string axion, one needs to have the domain wall formation later than the recombination era. Thus the prediction is the absence of the anisotropic birefringence from the CMB photon, but if the formation is well before the reionization, the anisotropy of the reionization photon birefringence can be obtained. Currently, the observational constraint on such anisotropic CB is still consistent even with the scenario with cosmic strings [90]. In addition, if the domain wall formed much before today, the gravitational waves can be emitted [91]. This is searched for together with the anisotropy of the CMB due to the gravitational potential of the domain wall [83, 92–94]. If the domain wall is just formed today, it does not reach the scaling solution, therefore we may have lots of domain wall balls with the size of  $1/m_\phi$ . This can be smaller than the size of the Universe given that the formation is after the epoch satisfying  $H \sim m_\phi$ . The photons from the (not too) far away galaxies can have the polarization rotation if they go through the wall by odd times. This rotation angle is predicted to be  $0.42c_\gamma$  deg, which is the twice of the isotropic CB of the CMB photon.

### 3 Time-Varying Dark Energy

As seen above, the late formation of domain walls is realized with the hilltop initial condition. When the axion remains around the hilltop and slowly rolls down the potential, it behaves as the dark energy component. Consequently, the late formation of the domain wall may result in time-varying dark energy.

To discuss it, one can again use the homogeneous scalar field in a large domain to simulate the system by using Eq. (15). Here we use  $H = H_0 \sqrt{\Omega_\Lambda + (V + \dot{\phi}^2/2)/(3M_{\text{pl}}^2 H_0^2) + \Omega_m(1+z)^3}$  with  $M_{\text{pl}} = 2.4 \times 10^{18}$  GeV being the reduced Planck mass, and  $H_0 \approx 68.5 \text{ km s}^{-1} \text{ Mpc}^{-1}$ ,  $\Omega_\Lambda \sim 0.7$ ,  $\Omega_m \approx 0.3$  [59]. We get the dark energy equation-of-state parameter

$$w_{\text{DE}} \equiv \frac{\dot{\phi}^2/2 - V - 3M_{\text{pl}}^2 H_0^2 \Omega_\Lambda}{\dot{\phi}^2/2 + V + 3M_{\text{pl}}^2 H_0^2 \Omega_\Lambda}. \quad (16)$$

The prediction for  $w_{\text{DE}}$  in terms of  $z$  is shown in Fig. 3, where we take  $f_\phi = 10^{15}$  GeV,  $\sigma_{\text{DW}} = (1 \text{ MeV})^3$ ,  $\phi_{\text{ini}} \approx 1 \text{ MeV}$ . While we evaluate  $w_{\text{DE}}$  using the homogeneous field, it will be spatially dependent because the axion oscillation is coherent only on subhorizon scales. Thus, the observed  $w_{\text{DE}}$  can be interpreted as the spatial average of  $w_{\text{DE}}$  over certain volumes. This should be not too different from the average of the homogeneous and oscillating  $w_{\text{DE}}$  over Hubble time.<sup>1</sup> One can see, unfortunately, that this parameter set cannot change the equation of state much (c.f. Fig. 4 for the DESI result).

On the other hand, in Fig. 4, we set  $f_\phi = 2.5 \times 10^{16}$  GeV,  $\phi_{\text{ini}} = 10^{13}$  GeV, and  $\sigma_{\text{DW}} = (5.1 \text{ MeV})^3$  for the red solid line together with the data point from the DESI DR2 [59]. Our prediction does not change  $z > 1$  behavior from the  $\Lambda$ CDM model.<sup>2</sup> The parameter choice for domain walls may be in tension with the domain wall problem. We note that the gravitational wave bound [91], for the early forming domain wall, does not affect our scenario. This is because the gravitational wave is being produced and is still weak (see the lattice simulation [95]). However, the usual bound on the anisotropy of the CMB photons may still exist in low momentum modes.<sup>3</sup> Although our scale-invariant fluctuations generate domain walls with a smaller area parameter [85], the constraint may be significant as well. However, if the formation is late we may be in a large void [39] due to the feature of the inflationary fluctuation making the constraint from the CMB anisotropy from the domain

<sup>1</sup>A more precise estimation using lattice simulations can also be performed.

<sup>2</sup>To get a better fit for  $z > 1$ , the change of the matter/radiation sector should be needed, which is model-dependent. We also note that the  $z < 1$  bin has the smallest error bar [59].

<sup>3</sup>The study of the impact on the CMB for forming domain walls is an interesting topic, which will be discussed in the future.

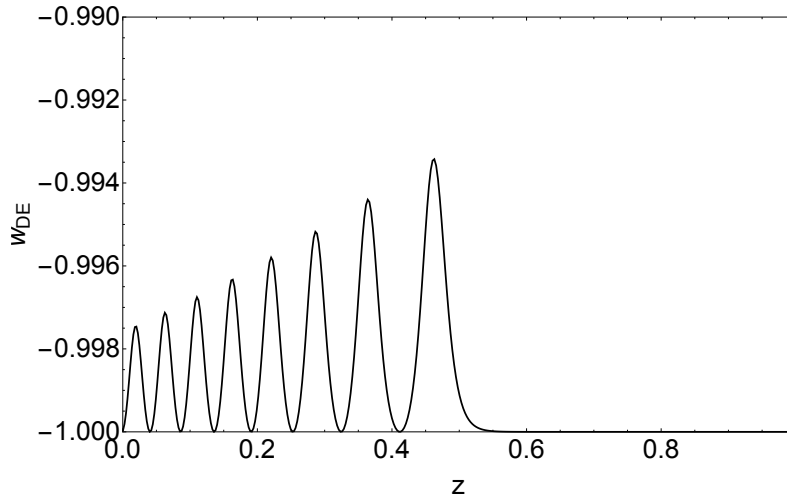


Figure 3:  $w_{\text{DE}}$  evolution in terms of  $z$  for the axion domain wall formation scenario. We take  $f_\phi = 10^{15}$  GeV,  $\sigma_{\text{DW}} = (1 \text{ MeV})^3$ ,  $\phi_{\text{ini}} = 1 \text{ MeV}$ .

wall highly alleviated. If one increases the tension (or equivalently the mass) by fixing the decay constant, the typical length  $1/m_\phi$  of the domain walls gets much smaller than the observable Universe, and the probability that our Universe is in the large void gets suppressed. Thus, again, the domain wall problem requires the formation of the domain wall at the late time.

Alternatively, for the large decay constant scenario we may introduce a very significant population bias, or even without considering the domain wall formation. The very large population bias is natural in the hilltop axion scenarios with stochastic initial distribution [79]. However, this may not explain why the scalar oscillation happens late.

The blue dashed line in Fig. 4 corresponds to the choice  $f_\phi = 2 \times 10^{14}$  GeV and  $\sigma_{\text{DW}} = (1 \text{ MeV})^3$ , with  $\phi_{\text{ini}}$  taken to be very close to the hilltop at an initial redshift of  $z = 1$ , leading to a significantly delayed onset of oscillation as can be seen in Fig. 2. This scenario requires some additional mechanism to realize such an initial condition. Such a mechanism can be found in, e.g., Refs. [39, 80, 96]. In this case, our scenario can give a better fit to the DESI data, while we need a slightly smaller decay constant for the string axion, which may require a large volume compactification. This can also be realized (see Ref. [46]). The prediction is a lot of small domain walls formed at  $z \lesssim 1$ . This could induce the birefringence of the photons from the distant galaxies.

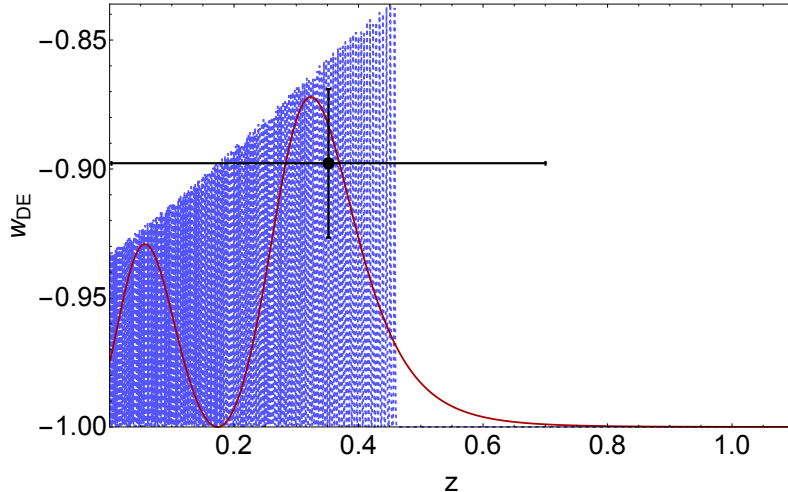


Figure 4: The same as Fig. 3 but we choose  $f_\phi = 2.5 \times 10^{16}$  GeV,  $\phi_{\text{ini}} = 10^{13}$  GeV,  $\sigma_{\text{DW}} = (5.1 \text{ MeV})^3$  for the red solid line. The blue dashed line denotes  $f_\phi = 2 \times 10^{14}$  GeV,  $\sigma_{\text{DW}} = (1 \text{ MeV})^3$ , with  $\phi_{\text{ini}}$  being located very close to the hilltop for the late onset of oscillation. The black point is the DESI DR2 result taken from Ref. [61].

## 4 Summary

In this paper, we have investigated the late-time formation of domain walls associated with the string axion as a natural explanation of the isotropic CB, which is motivated by the recent ACT DR6 results [17] and the previous analyses of the Planck and WMAP data [18–22].

Considering the cosmological domain wall problem, domain walls of the string axion should be formed well after the recombination (Fig. 1). Such late formation can be realized if the axion has a hilltop initial condition (Fig. 2). As a result, the isotropic CB angle is robustly predicted as  $\beta \approx 0.21c_\gamma$  deg, which agrees well with the recent ACT (and combined) result for  $c_\gamma \sim 1$ . While anisotropic CB is suppressed for the CMB photons from the recombination epoch due to the delayed domain wall formation, it is present for photons emitted at a later epoch. In addition, the domain walls themselves can induce the CMB anisotropies and gravitational waves.

Furthermore, we explored the implications of this scenario for time-varying dark energy, motivated by the recent DESI DR2 results [59], which further supports a deviation from a cosmological constant in addition to DESI DR1 [61]. We find that the equation-of-state parameter of dark energy can fit better the DESI results than the  $\Lambda$ CDM for low redshifts,  $z \lesssim 1$ .

In summary, our scenario highlights the intriguing possibility that late-time formation of domain walls associated with string axions could simultaneously explain isotropic cosmic birefringence and time-varying dark energy. To further assess the viability and testability of this scenario, future investigations on the CMB anisotropies, anisotropic CB, and gravitational waves will provide valuable insights, which we leave for future research.

## Acknowledgments

This work is supported by JSPS Core-to-Core Program (grant number: JPJSCCA20200002) (F.T.), JSPS KAKENHI Grant Numbers 20H01894 (F.T.), 20H05851 (F.T. and W.Y.), 22H01215 (W.Y.), 22K14029 (W.Y.), 23KJ0088 (K.M.), and 24K17039, (K.M.), Graduate Program on Physics for the Universe (J.L.) and JST SPRING Grant Number JPMJPS2114 (J.L.), Incentive Research Fund for Young Researchers from Tokyo Metropolitan University (W.Y.). This article is based upon work from COST Action COSMIC WISPers CA21106, supported by COST (European Cooperation in Science and Technology).

## References

- [1] E. Witten, *Phys. Lett. B* **149**, 351 (1984).
- [2] P. Svrcek and E. Witten, *JHEP* **06**, 051 (2006), [arXiv:hep-th/0605206](#) .
- [3] J. P. Conlon, *JHEP* **05**, 078 (2006), [arXiv:hep-th/0602233](#) .
- [4] A. Arvanitaki, S. Dimopoulos, S. Dubovsky, N. Kaloper, and J. March-Russell, *Phys. Rev. D* **81**, 123530 (2010), [arXiv:0905.4720 \[hep-th\]](#) .
- [5] B. S. Acharya, K. Bobkov, and P. Kumar, *JHEP* **11**, 105 (2010), [arXiv:1004.5138 \[hep-th\]](#) .
- [6] T. Higaki and T. Kobayashi, *Phys. Rev. D* **84**, 045021 (2011), [arXiv:1106.1293 \[hep-th\]](#) .
- [7] M. Cicoli, M. Goodsell, and A. Ringwald, *JHEP* **10**, 146 (2012), [arXiv:1206.0819 \[hep-th\]](#) .
- [8] M. Demirtas, C. Long, L. McAllister, and M. Stillman, *JHEP* **04**, 138 (2020), [arXiv:1808.01282 \[hep-th\]](#) .

- [9] J. Jaeckel and A. Ringwald, *Ann. Rev. Nucl. Part. Sci.* **60**, 405 (2010), [arXiv:1002.0329 \[hep-ph\]](#) .
- [10] A. Ringwald, *Phys. Dark Univ.* **1**, 116 (2012), [arXiv:1210.5081 \[hep-ph\]](#) .
- [11] P. Arias, D. Cadamuro, M. Goodsell, J. Jaeckel, J. Redondo, and A. Ringwald, *JCAP* **06**, 013 (2012), [arXiv:1201.5902 \[hep-ph\]](#) .
- [12] P. W. Graham, I. G. Irastorza, S. K. Lamoreaux, A. Lindner, and K. A. van Bibber, *Ann. Rev. Nucl. Part. Sci.* **65**, 485 (2015), [arXiv:1602.00039 \[hep-ex\]](#) .
- [13] D. J. E. Marsh, *Phys. Rept.* **643**, 1 (2016), [arXiv:1510.07633 \[astro-ph.CO\]](#) .
- [14] I. G. Irastorza and J. Redondo, *Prog. Part. Nucl. Phys.* **102**, 89 (2018), [arXiv:1801.08127 \[hep-ph\]](#) .
- [15] L. Di Luzio, M. Giannotti, E. Nardi, and L. Visinelli, *Phys. Rept.* **870**, 1 (2020), [arXiv:2003.01100 \[hep-ph\]](#) .
- [16] J. S. Reynés, J. H. Matthews, C. S. Reynolds, H. R. Russell, R. N. Smith, and M. C. D. Marsh, *Mon. Not. Roy. Astron. Soc.* **510**, 1264 (2021), [arXiv:2109.03261 \[astro-ph.HE\]](#) .
- [17] T. Louis *et al.* (ACT), (2025), [arXiv:2503.14452 \[astro-ph.CO\]](#) .
- [18] J. R. Eskilt and E. Komatsu, *Phys. Rev. D* **106**, 063503 (2022), [arXiv:2205.13962 \[astro-ph.CO\]](#) .
- [19] Y. Minami and E. Komatsu, *Phys. Rev. Lett.* **125**, 221301 (2020), [arXiv:2011.11254 \[astro-ph.CO\]](#) .
- [20] P. Diego-Palazuelos *et al.*, *Phys. Rev. Lett.* **128**, 091302 (2022), [arXiv:2201.07682 \[astro-ph.CO\]](#) .
- [21] J. R. Eskilt, *Astron. Astrophys.* **662**, A10 (2022), [arXiv:2201.13347 \[astro-ph.CO\]](#) .
- [22] J. R. Eskilt *et al.* (Cosmoglobe), *Astron. Astrophys.* **679**, A144 (2023), [arXiv:2305.02268 \[astro-ph.CO\]](#) .
- [23] S. M. Carroll, *Phys. Rev. Lett.* **81**, 3067 (1998), [arXiv:astro-ph/9806099](#) .

- [24] F. Finelli and M. Galaverni, *Phys. Rev. D* **79**, 063002 (2009), [arXiv:0802.4210 \[astro-ph\]](#) .
- [25] S. Panda, Y. Sumitomo, and S. P. Trivedi, *Phys. Rev. D* **83**, 083506 (2011), [arXiv:1011.5877 \[hep-th\]](#) .
- [26] M. A. Fedderke, P. W. Graham, and S. Rajendran, *Phys. Rev. D* **100**, 015040 (2019), [arXiv:1903.02666 \[astro-ph.CO\]](#) .
- [27] T. Fujita, Y. Minami, K. Murai, and H. Nakatsuka, *Phys. Rev. D* **103**, 063508 (2021), [arXiv:2008.02473 \[astro-ph.CO\]](#) .
- [28] T. Fujita, K. Murai, H. Nakatsuka, and S. Tsujikawa, *Phys. Rev. D* **103**, 043509 (2021), [arXiv:2011.11894 \[astro-ph.CO\]](#) .
- [29] F. Takahashi and W. Yin, *JCAP* **04**, 007 (2021), [arXiv:2012.11576 \[hep-ph\]](#) .
- [30] V. M. Mehta, M. Demirtas, C. Long, D. J. E. Marsh, L. McAllister, and M. J. Stott, *JCAP* **07**, 033 (2021), [arXiv:2103.06812 \[hep-th\]](#) .
- [31] S. Nakagawa, F. Takahashi, and M. Yamada, *Phys. Rev. Lett.* **127**, 181103 (2021), [arXiv:2103.08153 \[hep-ph\]](#) .
- [32] G. Choi, W. Lin, L. Visinelli, and T. T. Yanagida, *Phys. Rev. D* **104**, L101302 (2021), [arXiv:2106.12602 \[hep-ph\]](#) .
- [33] I. Obata, *JCAP* **09**, 062 (2022), [arXiv:2108.02150 \[astro-ph.CO\]](#) .
- [34] W. W. Yin, L. Dai, and S. Ferraro, *JCAP* **06**, 033 (2022), [arXiv:2111.12741 \[astro-ph.CO\]](#) .
- [35] N. Kitajima, F. Kozai, F. Takahashi, and W. Yin, *JCAP* **10**, 043 (2022), [arXiv:2205.05083 \[astro-ph.CO\]](#) .
- [36] S. Gasparotto and I. Obata, *JCAP* **08**, 025 (2022), [arXiv:2203.09409 \[astro-ph.CO\]](#) .
- [37] W. Lin and T. T. Yanagida, *Phys. Rev. D* **107**, L021302 (2023), [arXiv:2208.06843 \[hep-ph\]](#) .
- [38] K. Murai, F. Naokawa, T. Namikawa, and E. Komatsu, *Phys. Rev. D* **107**, L041302 (2023), [arXiv:2209.07804 \[astro-ph.CO\]](#) .

- [39] D. Gonzalez, N. Kitajima, F. Takahashi, and W. Yin, *Phys. Lett. B* **843**, 137990 (2023), [arXiv:2211.06849 \[hep-ph\]](#) .
- [40] M. Galaverni, F. Finelli, and D. Paoletti, *Phys. Rev. D* **107**, 083529 (2023), [arXiv:2301.07971 \[astro-ph.CO\]](#) .
- [41] J. R. Eskilt, L. Herold, E. Komatsu, K. Murai, T. Namikawa, and F. Naokawa, *Phys. Rev. Lett.* **131**, 121001 (2023), [arXiv:2303.15369 \[astro-ph.CO\]](#) .
- [42] L. Yin, J. Kochappan, T. Ghosh, and B.-H. Lee, *JCAP* **10**, 007 (2023), [arXiv:2305.07937 \[astro-ph.CO\]](#) .
- [43] F. Naokawa and T. Namikawa, *Phys. Rev. D* **108**, 063525 (2023), [arXiv:2305.13976 \[astro-ph.CO\]](#) .
- [44] K. Murai, F. Takahashi, and W. Yin, *Phys. Rev. D* **108**, 036020 (2023), [arXiv:2305.18677 \[hep-ph\]](#) .
- [45] S. Gasparotto and E. I. Sfakianakis, *JCAP* **11**, 017 (2023), [arXiv:2306.16355 \[astro-ph.CO\]](#) .
- [46] N. Gendler, D. J. E. Marsh, L. McAllister, and J. Moritz, *JCAP* **09**, 071 (2024), [arXiv:2309.13145 \[hep-th\]](#) .
- [47] A. Greco, N. Bartolo, and A. Gruppuso, *JCAP* **10**, 028 (2024), [arXiv:2401.07079 \[astro-ph.CO\]](#) .
- [48] J. Lee, K. Murai, F. Takahashi, and W. Yin, *JCAP* **05**, 122 (2024), [arXiv:2402.09501 \[hep-ph\]](#) .
- [49] F. Naokawa, T. Namikawa, K. Murai, I. Obata, and K. Kamada, (2024), [arXiv:2405.15538 \[astro-ph.CO\]](#) .
- [50] J. Lee, K. Murai, F. Takahashi, and W. Yin, *JCAP* **10**, 038 (2024), [arXiv:2407.09478 \[hep-ph\]](#) .
- [51] K. Murai, *Phys. Rev. D* **111**, 043514 (2025), [arXiv:2407.14162 \[astro-ph.CO\]](#) .
- [52] D. Zhang, E. G. M. Ferreira, I. Obata, and T. Namikawa, *Phys. Rev. D* **110**, 103525 (2024), [arXiv:2408.08063 \[astro-ph.CO\]](#) .

- [53] J. Kochappan, L. Yin, B.-H. Lee, and T. Ghosh, (2024), [arXiv:2408.09521 \[astro-ph.CO\]](#) .
- [54] W. Yin, (2024), [arXiv:2412.19798 \[hep-ph\]](#) .
- [55] E. Komatsu, *Nature Rev. Phys.* **4**, 452 (2022), [arXiv:2202.13919 \[astro-ph.CO\]](#) .
- [56] S. M. Carroll, G. B. Field, and R. Jackiw, *Phys. Rev. D* **41**, 1231 (1990).
- [57] S. M. Carroll and G. B. Field, *Phys. Rev. D* **43**, 3789 (1991).
- [58] D. Harari and P. Sikivie, *Phys. Lett. B* **289**, 67 (1992).
- [59] M. Abdul Karim *et al.* (DESI), (2025), [arXiv:2503.14738 \[astro-ph.CO\]](#) .
- [60] M. Abdul Karim *et al.* (DESI), (2025), [arXiv:2503.14739 \[astro-ph.CO\]](#) .
- [61] A. G. Adame *et al.* (DESI), *JCAP* **02**, 021 (2025), [arXiv:2404.03002 \[astro-ph.CO\]](#) .
- [62] D. Rubin *et al.*, (2023), [arXiv:2311.12098 \[astro-ph.CO\]](#) .
- [63] T. M. C. Abbott *et al.* (DES), *Astrophys. J. Lett.* **973**, L14 (2024), [arXiv:2401.02929 \[astro-ph.CO\]](#) .
- [64] Y. Tada and T. Terada, *Phys. Rev. D* **109**, L121305 (2024), [arXiv:2404.05722 \[astro-ph.CO\]](#) .
- [65] W. Yin, *JHEP* **05**, 327 (2024), [arXiv:2404.06444 \[hep-ph\]](#) .
- [66] M. Cortés and A. R. Liddle, *JCAP* **12**, 007 (2024), [arXiv:2404.08056 \[astro-ph.CO\]](#) .
- [67] P. Mukherjee and A. A. Sen, *Phys. Rev. D* **110**, 123502 (2024), [arXiv:2405.19178 \[astro-ph.CO\]](#) .
- [68] A. Notari, M. Redi, and A. Tesi, *JCAP* **11**, 025 (2024), [arXiv:2406.08459 \[astro-ph.CO\]](#) .
- [69] X. D. Jia, J. P. Hu, S. X. Yi, and F. Y. Wang, *Astrophys. J. Lett.* **979**, L34 (2025), [arXiv:2406.02019 \[astro-ph.CO\]](#) .
- [70] A. Hernández-Almada, M. L. Mendoza-Martínez, M. A. García-Aspeitia, and V. Motta, *Phys. Dark Univ.* **46**, 101668 (2024), [arXiv:2407.09430 \[astro-ph.CO\]](#) .

- [71] W. J. Wolf, C. García-García, and P. G. Ferreira, (2025), [arXiv:2502.04929 \[astro-ph.CO\]](#) .
- [72] A. Chakraborty, P. K. Chanda, S. Das, and K. Dutta, (2025), [arXiv:2503.10806 \[astro-ph.CO\]](#) .
- [73] E. V. Linder, *Phys. Rev. Lett.* **90**, 091301 (2003), [arXiv:astro-ph/0208512](#) .
- [74] R. de Putter and E. V. Linder, *JCAP* **10**, 042 (2008), [arXiv:0808.0189 \[astro-ph\]](#) .
- [75] W. Yin, *Phys. Rev. D* **106**, 055014 (2022), [arXiv:2108.04246 \[hep-ph\]](#) .
- [76] J. Khoury, M.-X. Lin, and M. Trodden, (2025), [arXiv:2503.16415 \[astro-ph.CO\]](#) .
- [77] R. Daido, F. Takahashi, and W. Yin, *JCAP* **05**, 044 (2017), [arXiv:1702.03284 \[hep-ph\]](#) .
- [78] R. T. Co, E. Gonzalez, and K. Harigaya, *JHEP* **05**, 163 (2019), [arXiv:1812.11192 \[hep-ph\]](#) .
- [79] F. Takahashi and W. Yin, *JHEP* **10**, 120 (2019), [arXiv:1908.06071 \[hep-ph\]](#) .
- [80] S. Nakagawa, F. Takahashi, and W. Yin, *JCAP* **05**, 004 (2020), [arXiv:2002.12195 \[hep-ph\]](#) .
- [81] Y. Narita, F. Takahashi, and W. Yin, *JCAP* **12**, 039 (2023), [arXiv:2308.12154 \[hep-ph\]](#) .
- [82] R. T. Co, T. Gherghetta, Z. Liu, and K.-F. Lyu, *JHEP* **09**, 145 (2024), [arXiv:2407.12930 \[hep-ph\]](#) .
- [83] Y. B. Zeldovich, I. Y. Kobzarev, and L. B. Okun, *Zh. Eksp. Teor. Fiz.* **67**, 3 (1974).
- [84] A. Vilenkin, *Phys. Rept.* **121**, 263 (1985).
- [85] N. Kitajima, J. Lee, F. Takahashi, and W. Yin, (2023), [arXiv:2311.14590 \[hep-ph\]](#) .
- [86] P. A. R. Ade *et al.* (BICEP, Keck), *Phys. Rev. Lett.* **127**, 151301 (2021), [arXiv:2110.00483 \[astro-ph.CO\]](#) .
- [87] M. Tristram *et al.*, *Phys. Rev. D* **105**, 083524 (2022), [arXiv:2112.07961 \[astro-ph.CO\]](#) .

- [88] P. Campeti and E. Komatsu, *Astrophys. J.* **941**, 110 (2022), [arXiv:2205.05617 \[astro-ph.CO\]](#) .
- [89] G. Galloni, N. Bartolo, S. Matarrese, M. Migliaccio, A. Ricciardone, and N. Vittorio, *JCAP* **04**, 062 (2023), [arXiv:2208.00188 \[astro-ph.CO\]](#) .
- [90] T. Namikawa, *Phys. Rev. D* **111**, 023501 (2025), [arXiv:2410.05149 \[astro-ph.CO\]](#) .
- [91] R. Z. Ferreira, S. Gasparotto, T. Hiramatsu, I. Obata, and O. Pujolas, *JCAP* **05**, 066 (2024), [arXiv:2312.14104 \[hep-ph\]](#) .
- [92] L. Sousa and P. P. Avelino, *Phys. Rev. D* **92**, 083520 (2015), [arXiv:1507.01064 \[astro-ph.CO\]](#) .
- [93] A. Lazanu, C. J. A. P. Martins, and E. P. S. Shellard, *Phys. Lett. B* **747**, 426 (2015), [arXiv:1505.03673 \[astro-ph.CO\]](#) .
- [94] N. Ramberg, W. Ratzinger, and P. Schwaller, *JCAP* **02**, 039 (2023), [arXiv:2209.14313 \[hep-ph\]](#) .
- [95] N. Kitajima, J. Lee, K. Murai, F. Takahashi, and W. Yin, *Phys. Lett. B* **851**, 138586 (2024), [arXiv:2306.17146 \[hep-ph\]](#) .
- [96] S. Nakagawa, F. Takahashi, M. Yamada, and W. Yin, *Phys. Lett. B* **839**, 137824 (2023), [arXiv:2210.10022 \[hep-ph\]](#) .